Structure of Metallic Hydrogen at Zero Pressure

E. G. Brovman, Yu. Kagan, and A. Kholas

I. V. Kurchatov Institute of Atomic Energy

Submitted May 12, 1971

Zh. Eksp. Teor. Fiz. **61**, 2429–2458 (December, 1971)

The properties of metallic hydrogen at atmospheric pressure are considered. The problem may be of great theoretical and practical importance. Perturbation theory is employed, which previously was successfully used for analysis of nontransition metals and which takes into account electron-ion interaction up to the third order inclusively. In the given case third-order terms were found to be very essential. It is found that metallic hydrogen tends to crystallize at P=0 into sharply anisotropic structures. This tendency in turn leads to the existence of a whole family of structures with very close energies. All Bravais lattices and the most important two-atom lattices are analyzed. It is found that minimum energy is possessed by a triangular family generated by a primitive hexagonal lattice and yielding a triangular filamentary structure with two-dimensional periodicity. The elastic properties and phonon spectrum of the structure are determined and local stability of the corresponding metastable phase is proven. The properties of metallic hydrogen under pressure will be considered in a separate paper.

1. INTRODUCTION

THE problem of metallic hydrogen has been attracting attention for a long time. Interest in it was initially connected primarily with astro-physical problems. Recently, however, this problem has also acquired a purely "terrestrial" interest, dictated mainly by two circumstances. First, hopes were raised that the technical problem of effecting under laboratory conditions the tremendous pressure necessary for the formation of the metallic phase of hydrogen would be solved in the nearest future. Second, a number of interesting aspects of the use of metallic hydrogen have been revealed, particularly, for example, in connection with the assumption that this state will have high-temperature superconductivity with T_c exceeding by several times the values for all presently known superconductors.

Wigner and Huntington[1] were apparently the first to state that the molecular hydrogen phase which is stable under normal conditions should go over into the metallic phase at very high pressure. In subsequent years, a whole series of papers was published[2-7], in which an attempt was made to find the thermodynamic potentials of the molecular and metallic phases of hydrogen as functions of the density and to determine from them the transition pressure p*. The limited accuracy of the approximations assumed in these papers has led to a noticeable spread in the critical pressures obtained by different authors.

In addition to these papers, a series of articles was also published, in which different physical properties of the metallic phase of hydrogen under pressure were analyzed. Mention should be made above all here of the work of Abrikosov[8-10]. Recently published papers are devoted to estimates of the temperature of the superconducting transitions for metallic hydrogen (Ashcroft[11] and Schneider and Stoll[12]).

There is no doubt that hydrogen becomes a metal under high pressure. However, even judging from the papers devoted to the calculation of the thermodynamic potential of the metallic phase in a crude structureless approximation (a detailed discussion is given below) we might assume that the plot of E against the volume Ω at $r_s \sim 1.6$ should have, in all probability, a stationary point $\partial E/\partial\Omega = -P = 0$, so that it is not excluded in principle that there exists a metallic state of hydrogen at atmospheric pressure. It corresponds, however, to an energy lying much above the energy of the ground state of the molecular phase at P = 0 (and the densities of the two phases differ by almost one order of magnitude), and therefore the metallic phase will in this case naturally be metastable. An analysis of the actual realizability of such a metastable phase of hydrogen, which is actually of prime significance for all "terrestrial" applications, presupposes the solution of an entire series of interrelated problems.

1. Determination of the energy of the metallic state of hydrogen and the proof of the existence of a stationary point with respect to all the parameters characterizing the phase, and also the determination of the crystal structure corresponding to the lowest possible energy at P = 0.

2. Proof of the stability of such a phase. It should include a test for dynamic stability, and furthermore both in the long-wave limit and at excitations with arbitrary wavelength (reality of the phonon frequencies for the entire momentum space), and also a verification of the stability of the phase relative to thermal fluctuations.

3. Determination of a relation between the structure obtained at a pressure corresponding to the phase transition from the molecular to the metallic phase, and the structure of a metastable phase at atmospheric pressure (generally speaking the two structures need not necessarily coincide, and also an analysis of the processes occurring when the pressure is removed.

4. A determination of the lifetime of the metastable state (which should also include an analysis of the possible existence of a metastable phase at $P < P^*$).

With all these questions answered in the affirmative, it would remain to solve yet another much more "pleasant" problem—determination of the phonon spectrum for this phase and, on its basis, knowing the electron-phonon interaction, estimation of the temperature of the superconducting transition.

To analyze the first two of the foregoing problems, it is necessary to solve the rather unique problem of finding the absolute minimum of the energy of the metallic phase (it is assumed that $T = 0$)

$$E = E(\Omega_0, \gamma_i) \tag{1.1}$$

as a function of the unit-cell parameters γ_i (we have explicitly separated one parameter, the atomic volume Ω_0). The problem of finding the optimal structure at a known Hamiltonian of interaction of all the particles making up the medium, and with complete absence of a priori information, is raised actually in such general form for the first time.

It must be emphasized that if the obtained phase corresponds to a minimum with respect to all the parameters in (1.1), then it automatically has long-wave dynamic stability. Indeed, positiveness of the corresponding quadratic form determines the stability of the phase relative to any type of homogeneous deformation, including with respect to a displacement of the sublattices relative to one another, if there is more than one ion per unit cell. If the minimum of the energy is sought on a class of structures with one atom per unit cell, then the energy depends on six variables (the number of independent parameters defining the unit cell), and in the notation of (1.1), if $P = 0$, there are in the general case five independent parameters γ_i. In such a five-dimensional space, points correspond to cubic crystals, lines to a family of uniaxial crystals, planes to rhombic crystals, etc.

A theoretical determination of the energy of the metallic phase for different values of the parameters γ_i is a very delicate problem. The point is that we encounter the need for calculating small differences that result from the change of the configuration of the protons against the background of much larger volume contributions. Therefore the traditional single-particle methods of band theory or methods of the Wigner-Seitz type, in which it is precisely the structural part of the energy which is poorly calculated, are practically hopeless.

In this connection we regard as most adequate for the problem the theoretical scheme developed in[13-16] and used to determine the properties of nontransition metals (see, for example,[17,18]). It is based on the possibility of writing down, in the absence of overlap between the ionic cores, the explicit form of the many-particle Hamiltonian of the electron-ion system of the metal, and presupposes determination of the energy and of the remaining physical quantities in the form of a series in powers of the electron-ion interaction, which actually represents a series in powers of the small ratio V_K/ϵ_F (V_K is the Fourier component of the electron-ion interaction at a momentum transfer equal to the reciprocal-lattice vector $K \neq 0$). The configuration part of the electron energy, which corresponds to the series terms containing the electron-ion interaction in the second and higher degrees, is then separated directly (as is also the energy of the ion lattice, which, naturally, depends on the configuration of the ions and the determination of which entails no fundamental difficulties).

Of very great importance for the developed theory is the possibility of going outside the framework of an approximation equivalent to allowance for only the term quadratic in the electron-ion interaction. The point is that an account of the higher-order terms is fundamental for the analysis of many properties (see, for example,[15,16]) and significantly alters also the purely quantitative picture, as is clearly demonstrated by direct calculations of the properties of metals (see, for example,[18]). In this case it is the third-order terms that are singled out. This is connected with the appreciable cancellation of the contribution made to the energy by the ion lattice and by the part of the electron energy which is quadratic in the interaction[14,18]. The role of the higher-order terms turns out, as a rule, to be weak.

When this scheme is used in the case of metallic hydrogen, we encounter a number of simplifying circumstances.

First, there is no problem of overlap of electron cores, since the latter are completely absent.

Second, the uncertainty in the value of the electron-ion interaction, which is inevitable in metals, is now eliminated, since the interaction now has a pure Coulomb character. (As a result, the problem has no free parameters at all, and includes only universal constants). As to the small parameter noted above, it can therefore easily be estimated:

$$\frac{V_K}{\varepsilon_F} = \frac{4\pi e^2}{K^2\Omega_0}\frac{1}{\varepsilon_F}, \tag{1.2}$$

and for K_{min} ($r_s \sim 1.6$) it turns out to equal $\sim 1/5$, i.e., is approximately the same as in the case of ordinary multivalent nontransition metals.

Third, the rough approximation used for description of the polarization operator and of the three-pole diagram corresponding to three-ion interaction via conduction electrons (see, for example,[18]), becomes more accurate the higher the electron density, and consequently it operates better in the metallic phase of hydrogen than in ordinary metals. As will be shown below, inclusion of third-order terms in the case of metallic hydrogen is even more fundamental in character than in the case of ordinary metals. A perturbation theory which takes only the second order into account leads, when the zero-point oscillation energy is taken into account, to a near-zero or even positive value of the adhesion energy, which makes the lattice unstable against disintegration into atoms.

Naturally, the use of a perturbation theory neglecting fourth-order terms entails a certain inaccuracy. It is very difficult to estimate realistically the resultant error in the determination of the different physical quantities. However, all the calculations of properties of non-transition metals within the framework of this approximation, and their comparison with experimental results for a large circle of static and dynamic characteristics, including the equation of state in the entire interval of accessible pressures and the phonon spectrum in the entire phase volume, give grounds for hoping that it will be small. This concerns, in particular, the determination of the relative change of the physical quantities on a change in the parameters of the structure, which properly speaking, is the main point in our paper.

Actually the only paper where account was taken of

the structure of metallic hydrogen was that by Schneider[7], in which the calculation scheme corresponds, in principle, to allowance for only second-order terms in the electron-ion interaction. One can make a few remarks with respect to the theoretical part of this paper, since some of the approximations mentioned by Schneider are in fact missing in a consistent many-particle theory. For example, there is actually no neglect in the "nonlocal character of the interaction" (using Schneider's terminology[7]); the nonadiabaticity, as is now well known[13], gives rise to a negligible correction to the energy and amounts to $\sim(\omega/\epsilon_F)^2$ of the vibrational energy. As to the results of his calculations, Schneider[7] has considered only one particular form of the structure (hexagonal close-packed lattice) which, as will be shown below, does not, on top of everything else, realize an absolute minimum of the energy at P = 0.

The present paper is devoted to a determination of the structure of the metallic phase of hydrogen at P = 0 and to a discussion of its properties. We used the already mentioned scheme of[13-18], in which the electron-ion interaction was taken into account to third-order terms inclusive and we obtained the absolute minimum of the energy (1.1) in the six-dimensional space of the parameters corresponding to lattices with one atom per unit cell. For cubic, uniaxial, and rhombic lattices, (for all 11 Bravais lattices) the problem was analyzed in the entire range of variation of the parameters. For structures having a lower symmetry, the Monte Carlo method in six-dimensional parameter space was used in the analysis.

We considered simultaneously also the known types of symmetrical lattices with two ions per unit cell, namely lattices of the diamond, white tin, and hexagonal close-packed types.

The analysis of the results has shown that the metallic-hydrogen phase most favored energywise has a unique structure which can be visualized as a system of proton filaments forming a rigid triangular lattice in a plane perpendicular to them and actually moving freely relative to one another in the direction along the filaments. Thus, we are dealing with a three-dimensional system having a two-dimensional periodic symmetry.

The question of the equation of state for the different phases and the character of the transition under pressure will be considered separately in a second part of the paper (to be published).

2. THE ENERGY OF THE METALLIC PHASE

By virtue of the validity of the adiabatic approximation, the energy of the metallic phase can always be represented as a sum of static and vibrational energies:

$$E_t = E + E_{vib}. \tag{2.1}$$

In the region of densities of interest to us, where P = 0, the energy is determined to a decisive degree by the static contribution. On the other hand, E_{vib}, being an integral characteristic of the vibrational spectrum, varies smoothly with changing ion configuration, and the density corresponding to P = 0 depends little on the structure. Therefore our search for optimal structures will be based on an analysis of the static part of the energy E, and only at the conclusion will we determine E_{vib} directly for minimal-energy structures.

The total static energy of the metal at T = 0 can be represented in the form of a series in the powers of the electron-ion interaction:

$$E = E_i + E_e,\ E_e = E^{(0)} + E^{(1)} + E^{(2)} + E^{(3)} + \dots \tag{2.2}$$

Here E_i is the energy of the ion lattice placed in a homogeneous negative background. For a proton lattice (Z = 1)

$$E_i = \frac{1}{2}\frac{e^2}{r_0}\alpha_M = \frac{\alpha_M(\gamma_i)}{r_s}\ (\text{Ry}). \tag{2.3}$$

We have introduced here the standard symbol r_S for the dimensionless radius of the sphere corresponding to the atomic volume Ω_0, expressed in Bohr radii, $\Omega_0 = \frac{4}{3}\pi r_0^3 = \frac{4}{3}\pi r_S^3 a_B^3$, and the Madelung constant α_M, which depends on the ion configuration. The energy (2.3), like the subsequent expressions, pertains to one ion and is expressed in Rydbergs. $E^{(0)}$ is the energy of the homogeneous electron gas:

$$E^{(0)} = \frac{3}{5}\frac{1}{\alpha^2 r_s^2} - \frac{3}{2\pi}\frac{1}{\alpha r_s} + \varepsilon_{corr}(r_s), \tag{2.4}$$
$$\alpha = (4/9\pi)^{1/3} \approx 0.521.$$

In the Nozieres-Pines approximation[19]

$$\varepsilon_{corr}(r_s) \approx -0.115 + 0.031 \ln r_s. \tag{2.4'}$$

From (2.4') we can easily conclude that in the range of variation of r_S of interest to us the inaccuracy in the determination of the correlation energy has practically no influence on the determination of the optimal structure and of the equilibrium value of the density.

Inasmuch as the electron-ion interaction is purely Coulomb in this case, there is no constant term b in the potential, connected with the presence of an electron[15,16], and accordingly

$$E^{(1)} = 0. \tag{2.5}$$

An exact expression for the electron contribution to the energy of second order in the electron-ion interaction[15,16] can be represented in the form

$$E^{(2)} = -27\alpha^4 \sum_{\mathbf{K}\neq 0} \frac{1}{(\mathbf{K}/K_F)^4}\frac{g(\mathbf{K})}{\varepsilon(\mathbf{K})}|S(\mathbf{K})|^2,$$
$$\varepsilon(\mathbf{K}) = 1 + \frac{9\alpha^4 r_s}{(\mathbf{K}/K_F)^2} g(\mathbf{K}). \tag{2.6}$$

Here K is the reciprocal-lattice vector, K_F the Fermi momentum ($K_F = 1/\alpha r_S a_B$), and S(K) the structure factor of the unit cell, and the dimensionless function g(K) coincides, apart from a factor, with the static polarizability of the electron gas:

$$\pi(\mathbf{K}) = \frac{3}{2}\frac{1}{\Omega_0 \varepsilon_F} g(\mathbf{K}).$$

In concrete calculations we used for g(K) the same approximation, in the spirit of Hubbard, which was used by us earlier in the analysis of the properties of metals[14,17,18], and which is widely used in contemporary calculations of the metallic state:

$$g(\mathbf{K}) = g_0(\mathbf{K}/K_F) / (1 - 9\alpha^4 r_s (\mathbf{K}/K_F)^{-2} f(\mathbf{K}/K_F) g_0(\mathbf{K}/K_F)), \tag{2.7}$$

$$g_0(x)=\frac{1}{2}+\frac{1-x^2/4}{2x}\ln\left|\frac{x+2}{x-2}\right|, \quad f(x)=\frac{1}{2}\frac{x^2}{x^2+\lambda}, \quad \lambda\approx 2.$$

The expression $E^{(3)}$ can be represented in the form[13-15]

$$E^{(3)}=-216\alpha^{10}r_s\sum_{\mathbf{K}_1\mathbf{K}_2\mathbf{K}_3\neq 0}\frac{S(\mathbf{K}_1)S(\mathbf{K}_2)S(\mathbf{K}_3)}{(\mathbf{K}_1/K_F)^2(\mathbf{K}_2/K_F)^2(\mathbf{K}_3/K_F)^2} \tag{2.8}$$
$$\times\frac{\tilde{\Lambda}^{(3)}(\mathbf{K}_1/K_F,\mathbf{K}_2/K_F,\mathbf{K}_3/K_F)}{\varepsilon(\mathbf{K}_1)\varepsilon(\mathbf{K}_2)\varepsilon(\mathbf{K}_3)}\Delta(\mathbf{K}_1+\mathbf{K}_2+\mathbf{K}_3)$$

(the coefficients of the sums in (2.6) and (2.8), when account is taken of the definition of α, are quantities of the order of unity).

The dimensionless three-pole $\tilde{\Lambda}^{(3)}$ is connected with the previosuly introduced three-pole $\Lambda^{(3)}$[15] by the simple relation

$$\tilde{\Lambda}^{(3)}=\Omega_0\varepsilon_F^2\Lambda^{(3)}. \tag{2.9}$$

In the calculations we used for $\Lambda^{(3)}$ the approximate three-pole value corresponding to a self-consistent definition of the energy of the free electron gas in the field of independently screened ions (see the corresponding expression, for example, in[18]).

At a fixed configuration, $\mathbf{K}/K_F$ and $S(\mathbf{K})$ do not depend generally on the density. On the other hand, even at the nearest lattice points, particularly in the case of a univalent metal, such as hydrogen is indeed, the dielectric constant no longer differs much from unity. By virtue of this we can conclude from (2.6)–(2.9) that at a fixed configuration $E^{(2)}$ is practically independent of the density r_s, while $E^{(3)}$ is proportional to r_s with good approximation. As to the dependence on the ion configuration, it becomes manifest in full measure in both terms $E^{(2)}$ and $E^{(3)}$, and also in E_i via the $\alpha_M(\gamma_i)$ dependence.

It is interesting that the weak dependence of $E^{(2)}$ on r_s makes it easy to obtain an a priori estimate of the equilibrium density corresponding to the condition $P=0$. To this end we determine the pressure in the so-called "zero model"[16], where the contribution of $E^{(2)}$ and $E^{(3)}$ is neglected completely (the contribution of $E^{(3)}$ to the pressure is certainly small compared with the contributions from E_i and $E^{(0)}$). In this approximation we have, consequently,

$$E\approx\frac{3}{5}\frac{1}{\alpha^2r_s^2}-\frac{3}{2\pi}\frac{1}{\alpha r_s}+\frac{\alpha_M}{r_s} \tag{2.10}$$

and accordingly the condition $P=0$, where

$$P=-\frac{\partial E}{\partial\Omega}=\frac{1}{4\pi a_B^3r_s^2}\frac{\partial E}{\partial r_s}$$
$$=\frac{1}{4\pi a_B^3r_s^3}\left[-\frac{6}{5\alpha^2r_s^2}+\frac{3}{2\pi}\frac{1}{\alpha r_s}-\frac{\alpha_M}{r_s}\right], \tag{2.11}$$

leads to the critical density

$$r_s^{(0)}=1.2/\alpha^2\left(\frac{1.5}{\pi\alpha}-\alpha_M\right). \tag{2.12}$$

Recognizing that α_M varies relatively little from configuration to configuration, we assume tentatively the value $\alpha_M=-1.8$, which corresponds to a spherical approximation (see, for example,[20]). This yields $r_s\sim 1.65$. For the compressibility κ we obtain in the "zero model"

$$\frac{1}{\kappa}=\frac{1}{3\pi a_B^3r_s^3}\left[\frac{3}{2}\frac{1}{\alpha^2r_s^2}-\frac{3}{2\pi}\frac{1}{\alpha r_s}+\frac{\alpha_M}{r_s}\right] \tag{2.13}$$

and, as can readily be seen, $1/\kappa>0$ (where $r_s\approx 1.65$).

As we shall see subsequently, the values (2.12) and (2.13) do not change greatly when account is taken of the structure-dependent terms. We can therefore assume that the presented simple estimates offer evidence of the existence of a density point that corresponds in the metallic phase to the condition $P=0$ and simultaneously to a positive compressibility, i.e., to stability with respect to change of volume at a fixed structure. It must be emphasized that, in contrast to an ordinary metal, this stationary point, and consequently the metallic bond, arise not as a result of competition between the contributions of E_i and $E^{(1)}$, but as a result of the competition of E_i and $E^{(0)}$, which leads to a much larger equilibrium density[16].

The question of the dependence of the system energy on the parameters γ_i characterizing the structure is much more complicated, and the solution of the problem of the optimal structure can be obtained only on the basis of a complete analysis of the behavior of the energy in multidimensional parameter space. Some general considerations, however, can be advanced even now.

The optimal-energy structure arises as a result of competition between the ionic and electronic terms $E^{(2)}$ and $E^{(3)}$. Although the term $E^{(2)}$ makes no practically no contribution to the pressure, its absolute value is comparable in magnitude with E_i (albeit smaller) at $r_s\sim 1.65$ and is noticeably larger than $E^{(3)}$. The qualitative features should therefore be revealed by a comparison of E_i and $E^{(2)}$.

From the form of expression (2.6), which contains a very sharp dependence on $\mathbf{K}$, it follows directly that by changing over to anisotropic structures we can decrease the energy $E^{(2)}$ (increase its absolute value). Indeed, at a fixed volume of the unit cell, the transition to sharply anisotropic structures leads to the occurrence of reciprocal-lattice points that lie in the region of small $\mathbf{K}$ and give accordingly a large contribution to $E^{(2)}$. The inevitable moving-aside of certain other reciprocal-lattice points has a much smaller effect, owing to the sharp decrease of $V_{\mathbf{K}}$ with increasing $\mathbf{K}$. We note that the term $E^{(3)}$ only intensifies this tendency. In particular, in $E^{(3)}$ there are contributions connected with the double scattering of the electron by the same ion, and these terms, together with $E^{(2)}$, form a term similar to (2.6), but with a scattering amplitude that is renormalized to become stronger.

On the other hand, the transition to anisotropic structures is inconvenient from the point of view of the ion energy, since it leads to an increase of E_i. Indeed, the parameter α_M in (2.3) has a maximum value for structures that are close to close-packed, and at a noticeable anisotropy it decreases continuously as the latter increases.

Which of these tendencies will prevail depends to a considerable degree on the density interval under consideration, since the role of E_i increases continuously with decreasing r_s. Thus, at $r_s\ll 1$ one can be assured that the energy minimum will correspond to symmetrical structures. At the density of interest to us, on the other hand, owing to the specific nature of the behavior of the Fourier component of the hydrogen potential, the tendency to anisotropy becomes manifest

to a much greater degree than in ordinary metals. Therefore, when searching for a structure that is optimal from the point of view of the energy, we cannot confine ourselves to an investigation of only the symmetrical structures that are usual for metals, and our analysis must include also sharply anisotropic lattices.

3. SEARCH FOR OPTIMAL STRUCTURE

In this section we present the results of a search for an optimal structure of metallic hydrogen. The investigation was carried out by successively increasing the number of parameters γ_i characterizing the structure. This has made it possible, in particular, to reveal clearly the instability tendencies that are characteristic of the system under consideration in different modifications, and approach purposefully the determination of the stable structure with minimum energy. To solve such a problem, it would be most important to choose parameters γ_i that specify the deformation of the unit cell in a form that is as convenient as possible, and furthermore for an arbitrary structure. It turns out that it is very convenient to introduce these parameters in the following manner (the connection with the usual strain tensor $\bar{u}_{\alpha\beta}$ is established with the aid of the relation $\bar{u}_{\alpha\beta} = \frac{1}{2}(u_{\alpha\beta} + u_{\beta\alpha})$; $u_{\alpha\beta} = \partial u_\alpha / \partial x_\beta$, for details see[21]):

$$1+u_{11} = (1+\gamma_1)^{1/3}(1+\gamma_2)^{-1/3}(1+\gamma_3)^{-1/2},$$
$$1+u_{22} = (1+\gamma_1)^{1/3}(1+\gamma_2)^{-1/3}(1+\gamma_3)^{1/2},$$
$$1+u_{33} = (1+\gamma_1)^{1/3}(1+\gamma_2)^{2/3},$$
$$u_{23} = \gamma_4, \quad u_{13} = \gamma_5, \quad u_{12} = \gamma_6, \quad u_{32} = u_{31} = u_{21} = 0. \tag{3.1}$$

We see therefore that γ_1 describes the change of the volume of the unit cell:

$$\Omega' = \Omega_0 \det(\delta_{\alpha\beta} + u_{\alpha\beta}) = \Omega_0(1+u_{11})(1+u_{22})(1+u_{33}) = (1+\gamma_1)\Omega_0. \tag{3.2}$$

The remaining γ_i describe pure shear deformations that conserve Ω_0. For example, γ_2 characterizes the change of (c/a) in uniaxial crystals:

$$\frac{c'}{a'} = \frac{x_3'}{x_1'} = \frac{(1+u_{33})x_3}{(1+u_{11})x_1} = (1+\gamma_2)\frac{c}{a}, \quad \frac{(c'/a')-(c/a)}{(c/a)} = \gamma_2. \tag{3.3}$$

Analogously, γ_3 describes the dilatation along the X_2 axis and the contraction along the X_1 axis at an unchanged length of the edge along X_3:

$$\frac{(b'/a')-(b/a)}{(b/a)} = \gamma_3. \tag{3.4}$$

The remaining three deformations have the meaning of "inclinations" of one axis to another:

$$x_2' - x_2 = \gamma_4 x_3, \quad x_1' - x_1 = x_3' - x_3 = 0 \tag{3.5}$$
$$x_1' - x_1 = \gamma_5 x_3, \quad x_2' - x_2 = x_3' - x_3 = 0, \tag{3.6}$$
$$x_1' - x_1 = \gamma_6 x_2, \quad x_2' - x_2 = x_3' - x_3 = 0. \tag{3.7}$$

We note that since the choice of (3.1) is in a certain sense arbitrary, we shall sometimes use other deformation parameters, namely in (3.5)–(3.7) we shall use the "inclination" in the opposite direction:

$$x_3' - x_3 = \gamma_4 x_2, \quad x_1' - x_1 = x_2' - x_2 = 0, \tag{3.8}$$
$$x_3' + x_3 = \gamma_5 x_1, \quad x_1' - x_1 = x_2' - x_2 = 0, \tag{3.9}$$
$$x_2' - x_2 = \gamma_6 x_1, \quad x_1' - x_1 = x_3' - x_3 = 0. \tag{3.10}$$

Now, expanding the lattice energy after deformation in a series, we obtain

$$(E' - E)/\Omega_0 = B_i\gamma_i + \tfrac{1}{2}B_{ij}\gamma_i\gamma_j + \ldots \tag{3.11}$$

It is precisely these moduli B_i and B_{ij} that can be obtained directly from calculations, and these, in turn, can then readily be connected with the usual elastic moduli C_i and C_{ij} (see[21]). (Expansion with the aid of $\gamma_{4'}$, $\gamma_{5'}$, and $\gamma_{6'}$ corresponds to the moduli B'_{ij}.)

Thus, the shape of the unit cell was specified with the aid of parameters γ_i that distort some primitive, say cubic, lattice. We considered initially single-parameter cubic crystals, then two-parameter uniaxial crystals, all three-parameter rhombic crystals, and finally the general case of a triclinic system. Inasmuch as cubic crystals are a particular case of uniaxial ones, we do not devote a separate section to them.

A. Uniaxial Lattices

Figure 1 shows the results of the calculation of the static energy as a function of the parameter c/a for all uniaxial Bravais lattices (i.e., assuming one ion per unit cell). In addition, the same dependence is given for two widely prevalent structures with two ions per unit cell—the β-Sn structure and the hexagonal close-packed structure. (In lattices where the Z axis coincides with the edge of the unit cell, the choice of c/a is obvious. For the rhombohedral structure, the Z axis was chosen along the three-dimensional diagonal, so that a simple cube, for example, corresponds to $c/a = 1/\sqrt{2}$.)

Each individual curve corresponds to a definite structure, marked by a figure on the right-hand side of the figure. The arrows designate especially the particular cases corresponding to single-parameter cubic lattices. All curves have been plotted under the additional condition (at each point relative to c/a)

$$\partial E/\partial\Omega_0 = 0, \tag{3.12}$$

so that different points on the curves correspond, in

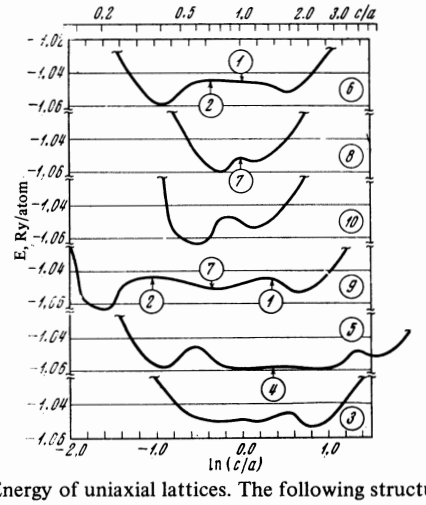

FIG. 1. Energy of uniaxial lattices. The following structures are marked: 1—face-centered cubic (FCC); 2—body-centered cubic (BCC); 3—hexagonal close packed (HCP); 4—diamond; 5—white tin, 6—face-centered tetragonal (FCT); 7—primitive cubic (PC); 8—primitive tetragonal (PT); 9—trigonal (rhombohedral) (RH); 10—primitive hexagonal (PH).

principle, to different densities. The extrema of the energy for each structure correspond to minima and maxima on the corresponding curves. It is important that by virtue of the symmetry of the structure and the condition (3.12), these minima and maxima are automatically extremal points with respect to all six parameters. Some of these extremal points correspond to more symmetrical cubic structures, for which stationarity with respect to (c/a) follows from symmetry, and others pertain to specifically two-parameter lattices. The question of whether a given extremum is a minimum with respect to other parameters must be solved separately every time, but for an analysis of single-parameter lattices Fig. 1 is already sufficient.

From the form of the curves we can immediately verify that all cubic structures are unstable. Indeed, a primitive cubic (PC) lattice corresponds to a minimum on the curve for the primitive tetragonal structure (PT); a body-centered lattice corresponds to maxima on the curves for face-centered tetragonal (FCT) and rhombohedral (RH) structures; a body-centered lattice corresponds to a maximum on the curve for the rhombohedral structure. A diamond-type lattice is also unstable, namely it corresponds to a maximum on the curve for the β-Sn structure. It is interesting that from the form of the presented curves one can incidentally draw qualitative conclusions concerning ordinary metals as well. For example, the character of the behavior of the curve for the PT lattice near the extremum corresponding to a PC lattice makes it possible to assume that in the case of indium, whose lattice has a tetragonal symmetry with a puzzlingly weak deviation of c/a from unity, we apparently encounter just such a situation (in the absence, of course, of a left-side minimum capable of competition).

Another interesting circumstance is the almost complete absence of a barrier between the BCC and FCC structures on the curve for the FCT lattice. This implies instability with respect to tetragonal distortion. It is important that this circumstance also prevails separately for the energy of the ion lattice in such a structure, and explains why one transverse elastic modulus $(C_{11} - C_{12})/2$ is anomalously small in metals of the Na type. It is possible that an analogous situation (a very weak barrier in a certain direction) is the cause of the low-temperature martensitic transition in these metals.

Analyzing the extrema belonging to already properly uniaxial structures, we must immediately call attention to the existence of an entire series of deep minima characterized each time by a strong structure anisotropy, namely, c/a differs strongly from unity. The smallest value of the energy is reached here in the primitive hexagonal (PH) and RH structures with $c/a < 1$, where the values of E are almost the same and amount to ≈ -1.063 Ry.

The presence of a deep minimum is evidence of the existence of stability with respect to one more parameter besides the density, namely with respect to c/a, corresponding to a large value of the modulus B_{22}. In order to analyze which of the obtained structures are stable with respect to all parameters γ_i, we found all the elastic moduli for the extremal points, and for

Table I

Structure	$(c/a)_0$	Ω_0/a_B^3	E, Ry/atom	Unstable moduli	"Soft" moduli
Face-centered tetragonal					
FCT (6)	0.399	18.96	−1.0591	—	(B_{44}), (B_{66})
BCC (2)	$1/\sqrt{2}$	17.91	−1.0453	B_{44}, (B_{22})	—
FCC (1)	1	17.90	−1.0459	B_{44}	(B_{22})
FCT (6)	1.642	18.58	−1.0523	(B_{33}), (B_{44})	(B_{66})
Primitive tetragonal					
PT (8)	0.793	19.07	−1.0587	—	B_{44}, (B_{66})
PC (7)	1	18.51	−1.0512	B_{22}	—
PT (8)	1.113	18.60	−1.0536	B_{33}	(B_{44}), (B_{66})
Primitive hexagonal					
PH (10)	0.593	20.83	−1.0631	—	B_{44}
PH (10)	1.107	18.48	−1.0536	—	B_{44}, (B_{66})
Rhombohedral					
RH (9)	0.198	20.82	−1.0631	—	B_{44}
BCC (2)	$1/\sqrt{8}$	17.91	−1.0453	B_{44}, (B_{22})	—
PC (7)	$1/\sqrt{2}$	18.51	−1.0512	B_{22}	—
FCC (1)	$\sqrt{2}$	17.90	−1.0459	B_{44}	(B_{22})
RH (9)	1.925	18.41	−1.0536	—	B_{44}, (B_{33}), (B_{66})
White tin (β-Sn)					
White tin (5)	0.397	19.03	−1.0588	(ω_c^2)	B_{44}, (B_{66})
White tin (5)	0.926	19.37	−1.0493	(B_{66}), ω_a^2	—
Diamond (4)	$\sqrt{2}$	19.97	−1.0583	B_{44}, (B_{22})	—
White tin (5)	4.583	18.60	−1.0528	B_{33}, B_{44}	ω_a^2
Hexagonal close-packed					
HCP (3)	0.764	18.53	−1.0508	B_{66}, ω_c^2	(B_{44})
HCP (3)	1.171	18.21	−1.0505	ω_a^2	(B_{44})
HCP (3)	2.217	18.40	−1.0535	(ω_a^2)	(B_{44}), (B_{66})

lattices with two ions per unit cell also both limiting frequencies of the optical phonons at $\mathbf{q} = 0$.

The results of such an investigation for all extremal points are gathered in Table I. This table indicates, besides the equilibrium values of $(c/a)_0$ and $(\Omega_0)_0$ and the values of the energy, also the unstable (negative) elastic moduli in explicit form. A separate column is devoted to the so-called soft moduli, i.e., elastic moduli which, while positive, are very close to zero (at least of the order of 10^{-2} of the compressibility modulus B_{11}). In the same two columns, the moduli with absolute values lower by one order of magnitude than B_{11} are given in the parentheses.

It can be concluded from the presented results that long-wave stability is possessed by anisotropic structures corresponding to both minima $c/a > 1$ and $c/a < 1$ for the PH and RH families, and minima with $c/a < 1$ for the PT, FCT, and β-Sn families. For all these structures there remains, however, the problem connected with the existence of one "soft" modulus, the modulus B_{44} in each case. The physical meaning of this will be explained in Sec. 4 on the basis of an analysis of the entire picture as a unit.

Besides the considered structures, it is necessary to single out also structures with "weak" instability; such structures are the FCT lattice at $c/a < 1$ and the HCP lattice at $c/a = 2.217$. These structures are characterized by the presence of only small negative moduli (in the case of the HCP lattice, an unstable homogeneous deformation turned out to be a displacement of the sublattices relative to each other, so that the square of the frequency of the limiting optical phonon with polarization in the basal plane, ω_a^2, is therefore negative). We have separated these modifications,

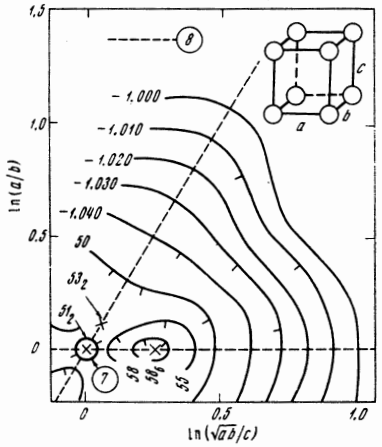

FIG. 2. Equal-energy levels for a family of primitive rhombic Bravais lattices.

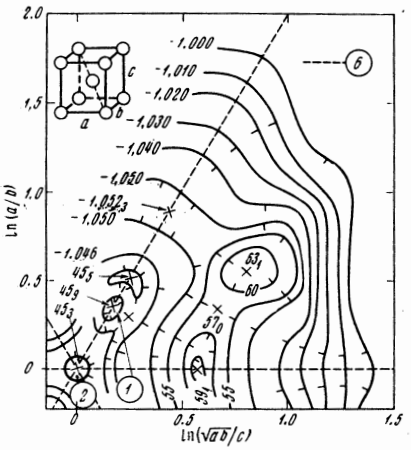

FIG. 4. Equal-energy levels for a family of body-centered rhombic Bravais lattices.

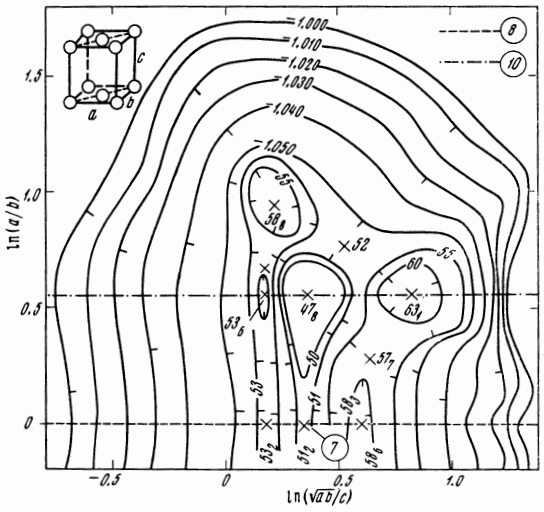

FIG. 3. Equal-energy levels for a family of rhombic base-centered Bravais lattices.

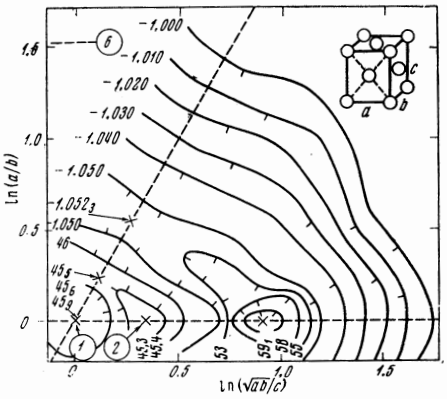

FIG. 5. Equal-energy levels for a family of face-centered rhombic Bravais lattices.

since one cannot exclude the possibility of their becoming stable under relatively small pressure.

B. Rhombic Lattices

The four rhombic Bravais lattices are already three-parameter structures. It is natural to choose, in addition to the density, also the ratio of the sides of the parallelepiped characterizing the lattice symmetry. Figures 2–5 show the constant-energy lines on the plane of these two parameters. The value at each point was obtained under the additional condition (3.12), so that the volume does not remain constant when moving along the constant-energy line or on going from one line to another. The same figures show the crystallographic cells and indicate especially how the parameters a, b, and c, the combinations of which are marked on the axes, are chosen. The figures show only the symmetry-irreducible part of the parameter plane, which amounts to one-sixth for the primitive (Fig. 2), body-centered (Fig. 4), and face-centered (Fig. 5) lattices. For a lattice with centered bases (Fig. 3) it amounts to one-half of the plane.

In the figures there are separated lines along symmetrical directions, corresponding to the uniaxial lattices already considered in Fig. 1. Thus, in Figs. 2 and 3 line 8 corresponds to the PT lattice, line 10 in Fig. 3 to the PH lattice, and line 6 in Figs. 4 and 5 to the FCT lattice. Naturally, with such a construction, it becomes possible to trace the evolution of the stability of lattices corresponding to extrema with respect to at least one deformation parameter, and particularly for the extrema shown in Fig. 1. Thus, on the PT line of Fig. 2 we see that the deepest minimum corresponds, besides large B_{22}, also to a rigid modulus B_{33} (deformation corresponding to a change of b/a), whereas it is clear from Fig. 3 that the modulus B_{66} (a deformation of the same type but in a different structure) should be relatively soft. On the FCT line, one can conclude for the deepest minimum from Fig. 5 that the modulus B_{33} is of the same scale as the rigid modulus B_{22}, and from Fig. 4 it can be concluded that the deformation corresponding to the change of b/a corresponds to a weak modulus, which in our nomenclature is B_{66}.

Let us now analyze the question as to which of the deepest energy minima are observed for rhombic structures. What is striking from the very outset is the absence of minima below the extreme ones obtained for uniaxial crystals. However, such a value at the minimum, $E = -1.063$, is observed not only at the obvious point corresponding to the PH line of Fig. 3, but also at the asymmetrical point on Fig. 4, corresponding to

Table II

Type of structure	$\ln(\sqrt{ab}/c)$	$\ln(a/b)$	Ω_a/a_B^3	E, Ry/atom	Stability
Base-centered rhombic	0.225	0.920	19.02	−1.0588	+
	0.530	0.760	18.85	−1.0520	−
	0.630	0.280	19.15	−1.0577	−
Body-centered rhombic	0.793	0.549	20.79	−1.0631	+
	0.660	0.350	19.76	−1.0575	−

the BCR lattice. The minima following them in depth turn out to be very close to those observed for tetragonal structures (E = −1.059). Here again, certain points are trivial, for example, the minima on the PT lines in Figs. 2 and 3 and on the FCT lines of Figs. 4 and 5. However, a minimum with the same value of the energy is also observed at a point of no definite symmetry, this time in Fig. 3.

In addition to the minima, the figures also show the saddle points, which are marked by crosses. All these points taken together represent the extremal values of the energy as a function of the six parameters. Table II gives the values of the parameters characterizing those extrema which were not previously involved in Table I. The last column of Table II designates the stability (plus) or instability (minus) of the corresponding structure with respect to all long-wave deformations.

We note in conclusion that the figures presented contain a large amount of information concerning the character of the possible instabilities. Thus, for example, from Fig. 4 we can deduce immediately that the second minimum on the FCT line is actually a saddle point and this structure is not separated by any energy barriers from the structure with the lowest value of the energy.

C. Triclinic Lattices

The next step was to consider lattices of arbitrary symmetry, i.e., the transition to the six-parameter space characteristic of the triclinic syngony. Since a regular analysis is practically impossible in this case, the Monte Carlo method was used. The random quantities were chosen to be the values of five parameters, and the sixth parameter, the density, was determined from the condition (3.12) for each set. Five convenient parameters were the logarithms of the ratios of the sides of the parallelepiped and the arctangents of the three angles characterizing the unit cell.

A random-number generator was used to choose directions in five-dimensional space, which were covered in equal steps, and the total energy E was calculated at each point. The motion was stopped only when the energy exceeded a certain limiting value and continued to grow continuously along the line, i.e., when we found ourselves clearly outside the region where deep minima are possible. Provision was made for further decrease in the calculation interval to be able to investigate all the local minima appearing during the course of motion along the line.

We investigated altogether 90 directions, and the energy was determined at approximately 1400 points of five-dimensional space. This has made it possible to trace quite thoroughly the entire potential relief in this space and to investigate a "valley" surrounded by "mountains" of height $E > -1.040$. We found 65 energy minima with $E < -1.055$, 26 minima with $E < -1.058$, and four minima with $E < -1.060$. To characterize the barriers, we note that the lowest maximum occurred at $E = -1.057$, and the highest one (in the "valley") at $E = -1.028$ (at two points). We used eight of the deepest minima (all four with $E < -1.060$ and four from the group with $E < -1.058$) as the starting points for the method of steepest descent (we used the improved variant of the method described in[22]). As a result we obtained local minima already in all the parameters, which in five cases led to close values of the energy, equal to $E \approx -1.063$. Three minima from the second group led to a value $E \approx -1.059$. All these eight cases are given in Table III, where the coordinates of the eight points are given in rectangular coordinates before and after using the method of steepest descent.

Table III

Number	Axis	Initial vectors a_1	a_2	a_3	E, Ry/atom	Final vectors a_1	a_2	a_3	E, Ry/atom	Number of variant
1	X	3.997	0,920	1.853		3.857	0.929	1.730		
	Y	0	1.819	−0 485	−1.06199	0	1.816	−0,390	−1.06313	109
	Z	0	0	2.867		0	0	2,970		
2	X	3,976	−0,624	0.809		3.834	−0.615	0.900		
	Y	0	3.952	1.062	−1.06087	0	3.975	1.209	−1.06307	601
	Z	0	0	1.422		0	0	1.368		
3	X	2.136	−1.162	0.330		2.041	−1.050	0.348		
	Y	0	3.218	1.698	−1.06097	0	3.424	1.715	−1.06308	619
	Z	0	0	2.880		0	0	2,970		
4	X	2.090	0.705	0.404		2.041	0,699	0.359		
	Y	0	3.209	1.570	−1.06130	0	3.430	1,714	−1.06313	721
	Z	0	0	3.018		0	0	2,973		
5	X	2.008	1.372	3.703		2.037	1.206	3,609		
	Y	0	6.010	2.717	−1,05839	0	5.951	2,972	−1.06308	710
	Z	0	0	1.771		0	0	1,720		
6	X	3.075	0.631	−0.080		3.034	0.731	−0.268		
	Y	0	2.170	−0,388	−1.05864	0	2.174	−0.900	−1.05900	205
	Z	0	0	2.874		0	0	2.878		
7	X	3.185	0,663	2,232		3.124	0,488	2,225		
	Y	0	3.088	−0.770	−1.05903	0	3.094	−0,780	−1.05909	222
	Z	0	0	1,932		0	0	1,962		
8	X	4.790	1,155	3.563		4.725	1.194	3,544		
	Y	0	4,599	2.701	−1.05892	0	4.537	2,707	−1.05910	602
	Z	0	0	0.870		0	0	0.884		

Table IV

Type of structure	Number of variant	ξ	η	E, Ry/atom
PH	—	0.000	0.000	−1.06310
RH	—	0.333	0.333	−1.06313
BCR	—	0.500	0.000	−1.06307
Triclinic	109	0.22	0.65	−1.06313
	601	0.83	1.03	−1.06307
	619	−0.52	0.69	−1.06307
	721	0.34	−0.17	−1.06313
	710	−2.96	+1.78	−1.06308

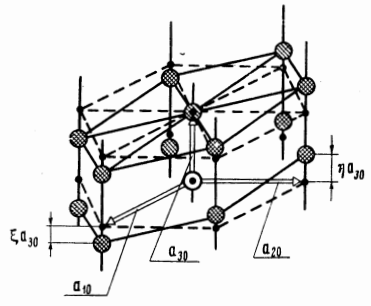

FIG. 6. Example of lattice belonging to the hexagonal two-parameter family.

It is interesting that no minima with energy lower than for the record-setting uniaxial lattices were observed among these values. The obtained five minima lie at arbitrary points of the space under consideration, i.e., they correspond to a triclinic system and have practically the same energy as the deepest minima of the two-parameter and three-parameter lattices. The three other minima have an energy that coincides in magnitude with the deepest minima of the tetragonal structures.

4. ANALYSIS OF RESULTS

An examination of the results obtained in the preceding section reveals the following interesting circumstance: the eight deepest minima corresponding to the different structures (one PH, one RH (Table I), one BC rhombic (Table II), and five triclinic (Table III)) correspond to very close values of the energy, within 5×10^{-5} Ry $\approx 10°$K. The next minima are separated from this family by an energy interval of 4×10^{-3} Ry $\approx 650°$K, i.e., the separation is of the same scale as that between different modifications for ordinary metals. Finally, the third type of stable minima (see Table I) follows at approximately another 800°K higher (we note that although these energy intervals are small compared with the total energy, they are nevertheless comparable in magnitude with the entire structure-dependent part of the energy, and consequently are reliably determined within the framework of the employed scheme).

Such a surprising degeneracy for structures that are at first glance entirely different in symmetry and correspond to minimum energy suggests the presence of a certain internal connection between them.

An attentive analysis of the crystallographic structure of the "record setting" lattices shows that this is indeed the case. All eight lattices can be obtained by starting from the primitive hexagonal lattice (it is also a member of the family) if the lattice points are shifted along the Z axis (parallel to C), but the hexagonal projection on the XY plane and the distance between the lattice points along the axis remain unchanged (see Fig. 6, which shows both the initial PH lattice and an example of the distorted lattice). Since the lattice must remain a Bravais lattice, it is easily understood that we have two independent possibilities for such distortion of the unit cell, by shifting through an arbitrary distance, for example, the chain of atoms passing through the ends of the vectors $\mathbf{a}_{10}$ and $\mathbf{a}_{20}$ (Fig. 6). We thus obtain a two-parameter family, which we shall describe by means of the relative shifts ξ and η. Denoting the basis vectors of the initial hexagonal lattice by $\mathbf{a}_{10}$, $\mathbf{a}_{20}$ and $\mathbf{a}_{30}$, we obtain for the basis vectors of the transformed lattice

$$\mathbf{a}_1 = \mathbf{a}_{10} + \xi\mathbf{a}_{30}, \quad \mathbf{a}_2 = \mathbf{a}_{20} + \eta\mathbf{a}_{30}, \quad \mathbf{a}_3 = \mathbf{a}_{30}. \tag{4.1}$$

It is clear that in terms of such coordinates the PH lattice corresponds to $\xi = 0$ and $\eta = 0$, while the RH lattice corresponds to $\xi = \eta = 1/3$. It is not directly obvious that the triclinic lattices belong to the family, and to check on this it is necessary to change over from the basis vectors given in Table III to the new axes X, Y, and Z. The results are given in Table IV. We note also that in all cases it was found that the volume of the unit cell, $\Omega_0 \approx 20.8\ a_B^3$, and the distance between ions along the Z axis, $d = 2.04a_B$, remain constant with high accuracy.

In order to verify that we are dealing with a continuous family of structures, we undertook a calculation of the energy for lattices with basis vectors (4.1) with regular variation of ξ and η. It is clear that, owing to the periodicity, it suffices to consider the region $0 < \xi$, $\eta < 1$, and since these are Bravais lattices, in general one-twelfth of this square is irreducible.

The energy values corresponding to the points ξ and η obtained by regular subdivision of the corresponding irreducible triangle are listed in Table V. It is seen from these data that the energy difference for different structures of the family does not exceed 10°K. Thus, on the basis of the results we can conclude that the minimum energy for the metallic phase of hydrogen indeed corresponds to a continuous family of structures of the type (4.1) with fixed distances between the atoms along the Z axis and with potential barriers within the family on the order of 10°K and below. Before we discuss other properties of this family, let us analyze the physical factors that give rise to it.

As noted in Sec. 2, an equilibrium structure is the

Table V

18ξ	18η	E, Ry/atom
0	0	−1.06310
3	0	−1.06311
6	0	−1.06311
9	0	−1.06307
2	2	−1.06312
5	2	−1.06312
8	2	−1.06310
4	4	−1.06313
7	4	−1.06315
6	6	−1.06313

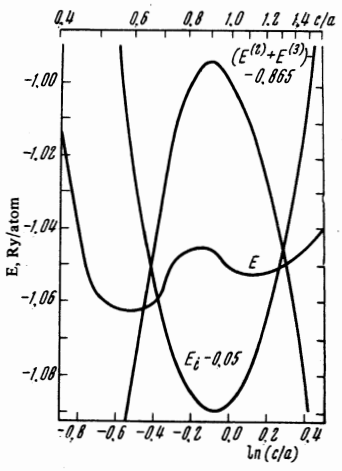

FIG. 7. Energy of primitive hexagonal lattice of metallic hydrogen as a function of c/a, Ω_0 = 20.8 a_B^3.

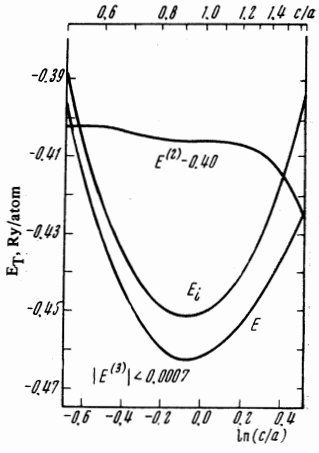

FIG. 8. Energy of primitive hexagonal lattice of sodium as a function of c/a, Ω_0 = 254 a_B^3.

result of competition between the ion-lattice energy E_i (2.3) and the structure-dependent part of the electron energy $E^{(2)} + E^{(3)}$ ((2.6) and (2.8)). The behavior of the first of these quantities calls for a tendency towards close-packed structures, whereas the electronic part of the energy is smaller the more anisotropic the structure. The tendency to anisotropy turns out to be stronger the larger the value of the Fourier component V_q of the electron interaction, at wave vectors on the order of the nearest reciprocal-lattice vectors if the density remains unchanged. In this sense, metallic hydrogen occupies a special place, since its V_q corresponds to ordinary Coulomb interaction and retains the same sign in the entire interval of variation of q, whereas for all nontransition metals the Fourier component of the pseudopotential passes through zero precisely in the interesting region of variation of q (see, for example,[23]). Therefore the gain due to the asymmetry causing the shift of some of the reciprocal-lattice points towards smaller q (see Sec. 2) in the case of ordinary metals turns out, as a rule, to be much less pronounced than in the case of hydrogen, and the structure there is governed decisively by the behavior of E_i.

In the case of metallic hydrogen, the picture is essentially different and the structure-dependent part of the electronic energy gives rise to sharply anisotropic equilibrium structures, as follows from all the previously obtained results. Incidentally, the tendency of the electronic energy towards anisotropic structures can be explained without resorting to (2.6), using the following simple reasoning: in an anisotropic metal the distances to certain reciprocal-lattice points, and consequently to the corresponding Brillouin planes, decrease. The energy gaps on these planes increase and "squeeze" the entire electron spectrum downward, increasing the total electron energy. (The distortion of the dispersion law near the gap in a univalent metal has in itself very little effect on the total energy, and can be obtained by perturbation theory, as was done above.)

To illustrate all the foregoing, Fig. 7 shows the total energy of the primitive hexagonal lattice of metallic hydrogen and individual contributions made to it as functions of c/a at a fixed density. For comparison, Fig. 8 shows the same curves for ordinary univalent metallic sodium with equilibrium density and with a pseudopotential taken from our earlier paper[17]. Curves analogous to those of Fig. 8 were obtained by us also for the PH lattice of Mg, although the contribution of the electron energy in this case is somewhat higher. For an HCP lattice these data are given in[18].

It is seen from the figures that the sharp growth of E_i as $c/a \to 0$ and $c/a \to \infty$, due to the coming together of the planes with like charges, always operates against very sharp deviations from unity. On the other hand, in the region $c/a \sim 1$ in the case of ordinary metals, the electronic part of the energy changes little and the minimum of the total energy is close to the minimum of the energy of the ion lattice ($c/a \approx 0.95$). To the contrary, in the case of hydrogen, when c/a deviates from the ideal value the decrease of the electronic energy in this region is faster than the increase of E_i, as a result of which the total-energy curve acquires two minima corresponding to strongly anisotropic structures. The deeper minimum corresponds to a lattice that is compressed along the Z axis, in which, in reciprocal space, six of the first lattice points, which are symmetrically disposed in the basal plane of the reciprocal lattice, are shifted much closer to K = 0, and two of the first points along the Z axis, to the contrary, are shifted to larger distances in comparison with the close-packed structure, where all eight points are at equal distances. Owing to the very strong decrease of the contribution from the individual reciprocal-lattice points with increasing K (see Sec. 2) the electronic contribution to the energy is determined principally precisely by these first six points in the basal plane. The second minimum, to the contrary, corresponds to a lattice that is elongated along the Z axis, in which it is precisely the first two points along the Z axis, which play in this case the decisive role, that are closer together in reciprocal space.

We note that a similar picture in the behavior of the total energy and of the individual contributions to it as functions of c/a can be traced also with two other structures of metallic hydrogen as examples (see Fig. 1), particularly tetragonal ones. At the same time, it is clear from general considerations that it is precisely in the hexagonal lattice that the gain in the electronic energy is maximal, since we are dealing with

Table VI

	d/a_B	E, Ry/atom	$B_1 = -P$	B_2	$B_{11} = B$	B_{22}	B_{12}	B_{33}	$B_{4'4'}$	B_{55}	B_{66}
Primitive hexagonal lattice											
$E^{(0)}$	2.038	0.12323	−22.4	—	42.0	—	—	—	—	—	—
$E^{(2)}$		−0.16191	0.4	16.8	−0.3	−38.9	−1.2	−4.4	0.3	—	—
$E^{(3)}$		−0.05612	−0.8	6.8	0.8	−21.9	0.5	11.1	0.3	—	—
E_i		−0.96830	22.8	−23.6	−30.4	86.3	7.9	17.4	−0.5	—	—
Sum		−1.06310	0.0	0.0	12.1	25.5	7.2	24.1	0.1	$\equiv B_{4'4'}$	B_{33}
Rhombohedral lattice											
$E^{(0)}$	2.040	0.12369	−22.4	—	42.0	—	—	—	—	—	—
$E^{(2)}$		−0.16140	0.4	16.9	−0.3	−38.2	−1.2	−4.4	−0.1	—	−4.4
$E^{(3)}$		−0.05590	−0.8	6.8	0.8	−21.9	0.5	11.0	0.2	—	11.0
E_i		−0.96952	22.8	−23.7	−30.4	85.4	7.9	17.3	0.2	—	17.3
Sum		−1.06313	0.0	0.0	12.1	25.3	7.2	23.9	0.3	$\equiv B_{4'4'}$	23.9
Rhombic lattice											
Sum	2.034	−1.06307	0	0	12.1	25.5	7.2	24.3	≈ 0	≈ 0	24.0

Note. Moduli in units of 10^{11} dyne/cm^2 = 100 kbar. The same for Tables VII and VIII. For the rhombic lattice, $B_{13} \approx 0$ and $B_{23} \approx 0$.

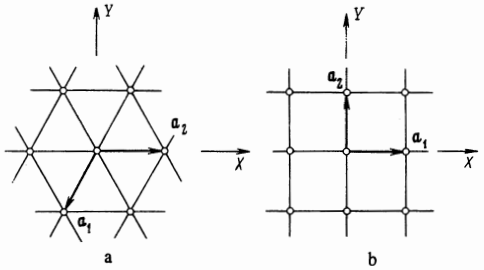

FIG. 9. Projection on the XY plane of lattices from the "triangular" (a) and "quadratic" (b) families.

six closest lattice points, and not with four as in the tetragonal case.

The situation, with the special role played by the six nearest reciprocal-lattice points lying in the basal plane, explains the appearance of an entire family of energywise-close structures. The point is that for all the members of the hexagonal family it is precisely the position of these nearest lattice points that remains constant, owing to the fact that in direct space the projection of the direct-lattice points on the XY plane forms one and the same triangular plane lattice (see Fig. 9a). If we denote by $\mathbf{b}_{10}$, $\mathbf{b}_{20}$, and $\mathbf{b}_{30}$ the reciprocal-lattice vectors for PH, then we have for family (4.1) the following values of the reciprocal-lattice basis vectors:

$$\mathbf{b}_1 = \mathbf{b}_{10}, \quad \mathbf{b}_2 = \mathbf{b}_{20}, \quad \mathbf{b}_3 = \mathbf{b}_{30} - (\xi\mathbf{b}_{10} + \eta\mathbf{b}_{20}). \tag{4.2}$$

Thus, on going from one member of the family to another, only the more remote lattice points, which make a small contribution to the electronic energy, are shifted. Noting in addition that, for the same reason, E_i for this family also changes very little (in other words, the distance between the ions in the XY plane is large compared with the distance along Z), then it becomes clear why these structures, which at first glance are so different, have anomalously close energy values.

We proceed now to an analysis of the dynamic characteristics of lattices from the hexagonal family. We consider first the long-wave properties determined by the elastic moduli. It was found already in the analysis of uniaxial lattices that two members of the family, corresponding to PH and RH lattices, have long-wave dynamic stability. A similar result was also obtained for the other members of the family. Table VI gives by way of an example the values of all the elastic moduli for three members of the family in the symmetric structures PH, RH, and BC rhombic, in the first two cases with complete breakdown of the contributions from the individual terms of the series (2.2). The striking result is here not only the close agreement between the values of all the corresponding moduli, but also of the individual contributions to them (the modulus $B_{4'4'}$ is discussed later on). Even the contributions to the modulus B_{66} coincide here with the contributions to B_{33} in RH, although from symmetry considerations they are equal only for hexagonal-symmetry lattices. The three additional moduli which appear in the rhombic structure are practically equal to zero.

Thus, the elastic properties of the rhombohedral and rhombic lattices would appear to put them in the more symmetrical hexagonal class. It is easily understood now that this is another manifestation of the microscopic picture outlined above, where the decisive role is played only by the six nearest reciprocal-lattice points, and therefore the elastic properties correspond not to the symmetry of the space group of the crystal, but to the hexagonal symmetry of the arrangement of these points. The statement that the individual contributions are equal pertains also to the energy as well as to the first-order moduli given in the first columns of the table, It is quite clearly seen here, in particular, that the condition $P = 0$ is indeed reached as a result of the contributions from E_i and $E^{(0)}$ (see Sec. 2), and that the equilibrium with respect to the parameter c/a ($B_2 = 0$) is due to the competition between $E^{(2)}$, $E^{(3)}$, and E_i, all the contributions being large (see Fig. 7), i.e., far from the stationary value of each contribution.

The most interesting result that follows from the presented table is that in all three structures the same modulus, $B_{4'4'}$, turns out to be smaller by two orders of magnitude than the remaining moduli. This modulus is defined (see above) as the second derivative with respect to $\gamma_{4'}$ of the energy for the shear deformation (3.8). It is easy to visualize that in such a definition of the deformation, the smallness of the modulus $B_{4'4'}$ reflects precisely the very small energy change following a distortion corresponding to a transition to other

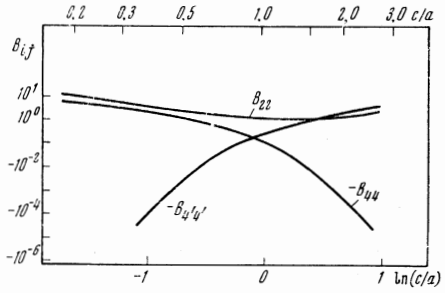

FIG. 10. Ionic contribution to the elastic moduli B_{22}, B_{44}, and $B_{4'4'}$ as functions of c/a for primitive hexagonal lattice. c/a = 0.59 for the case P = 0.

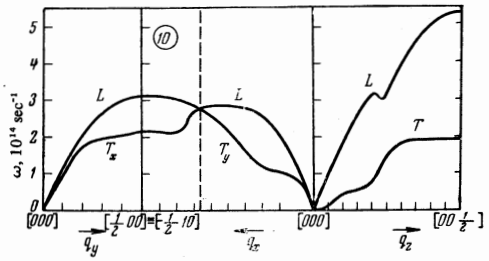

FIG. 11. Phonon spectrum for primitive hexagonal lattice of metallic hydrogen, $\Omega_0 = 20.1 a_B^3$, c/a = 0.596.

members of the family via a small displacement. Thus, the existence of a family of structures with very close energies and the presence of an anomalously "soft" modulus are two aspects of one and the same physical picture.

It is important to emphasize that it is not only the modulus $B_{4'4'}$ itself that is anonamously small, but also the individual contributions to it, a fact that can be understood, incidentally, already from the close values of the individual contributions to the energy for different members of the family (see Table VI). In Fig. 10 we have shown the contribution made to $B_{4'4'}$ by the ion lattice at a fixed density for PH, and for the sake of comparison also the same dependence for the modulus B_{22}. We see that with increasing anisotropy, the value of this contribution of $B_{4'4'}$ decreases exceedingly rapidly, in full agreement with the physical considerations advanced above. It should be noted that the absolute value of $B_{4'4'}$, for all the members of the family, is determined with a relatively large error, which is natural if it is recognized that the change corresponds to motion along an energy relief with fluctuations on the order of only 10°K. Therefore, strictly, speaking, one can only state that $B_{4'4'} \approx 0$.

To analyze the overall dynamic stability, it was necessary to find the phonon spectrum for the entire phase space of the wave vectors. To this end, we constructed the dynamic matrix of the oscillations, with allowance for third-order terms in the electron-proton interaction (see, for example,[18]) and obtained the spectrum for two members of the family—the PH and RH structures. In both cases, the spectrum turned out to be stable, i.e.,

$$\omega_\alpha^2(q) \geqslant 0 \qquad (4.3)$$

for all wave vectors q and all modes α.

Figure 11 shows the phonon spectrum of a primitive hexagonal lattice for three symmetrical directions of the wave vector. The two transverse oscillation modes with polarization along Z, one with q along q_x and the other with q along q_y, turn out to be anomalously low in the entire interval of variation of q, and were not shown at all in Fig. 11, since the accuracy with which these frequencies are determined is extremely low (for the same physical reasons as $B_{4'4'}$, and see also below). These are the same modes for which the initial section of the spectrum determines the speed of sound, which is connected with the modulus $B_{4'4'}$. We see that not only under uniform deformation corresponding to the elastic moduli, but also under a small relative displacement of close chains along Z, the energy changes very little, corresponding to near-zero values of the excitation energy.

It is interesting that, owing to symmetry, the modulus $B_{4'4'}$ also determines the velocity of transverse sound in the propagation of a phonon along q_Z, and this velocity is thus also anomalously low. However, at noticeable values of q, the distortion caused by such a wave is in no way "easy," and accordingly, the phonon frequencies assume the usual orders of magnitude.

For a rhombohedral structure, the phonon frequencies turned out to be practically the same, and all the results described above remain in force.

The entire discussion in the present section has pertained so far to Bravais lattices, i.e., lattices with a single atom per unit cell. In particular, as we have seen, an easy motion, which transforms one member of the hexagonal family into another, corresponds to arbitrary shifts of chains of atoms along the Z axis, but the lattice remains monatomic, which, of course, imposes stringent limitations on the shifts of the other chains along the Z axis.

However, on the basis of the microscopic analysis given above, one can assume that if a polyatomic lattice is produced as a result of distortion, but the nearest reciprocal-lattice points remain the same, then the energy of the new lattice should again differ very little from the initial one. By way of illustration, let us consider the following two-atom lattice. Let the cell along the a_{20} axis double compared with the initial PH lattice:

$$\mathbf{a}_1 = \mathbf{a}_{10}, \quad \mathbf{a}_2 = 2\mathbf{a}_{20}, \quad \mathbf{a}_3 = \mathbf{a}_{30}$$

and let a second atom appear in the unit cell:

$$\rho_1 = 0, \quad \rho_2 = \mathbf{a}_{20} + \lambda \mathbf{a}_{30}.$$

Then, as can readily be seen, we have for the reciprocal-lattice vectors

$$\mathbf{b}_1 = \mathbf{b}_{10}, \quad \mathbf{b}_2 = \mathbf{b}_{20}/2, \quad \mathbf{b}_3 = \mathbf{b}_{30}.$$

Thus, we get "extra" reciprocal-lattice points in the basal plane, for example $\mathbf{b}_{20}/2$. It must be remembered, however, that in a two-atom lattice the potential in the expression for the energy (2.6), (2.8) is multiplied by a structure factor $(\frac{1}{2})[1 + \exp(i\mathbf{K}\rho_2)]$. It is easy to see that this structure factor precisely "extinguishes" the contribution from the point $\mathbf{b}_{20}/2$. At the same time, new lattice points, not cancelled out by the structure factor, do indeed occur in the next plane along Z, for example $(\mathbf{b}_{20}/2) + \mathbf{b}_{30}$. The energy of the new lattice is different by precisely the amount

of the contribution of these remote lattice points, and thus depends on the parameter λ, but very weakly. To verify this, we have performed a direct calculation of the energy of such two-atom lattices. The calculation has confirmed the assumption fully and yielded for the energy difference a value on the order of 10°K. A similar conclusion can be drawn also for the case of polyatomic lattices.

Thus, the family of "optimal" structures also includes polyatomic lattices of the type described. This allows us to draw the important conclusion that the energy of such structures remains unchanged, with the same accuracy as before (~10°K), even after arbitrary relative motion of all the atom chains, provided a fixed triangular lattice is conserved in the projection on the XY plane. (As to the phonons, of course, additional optical modes arise when the cell is doubled, and the optical oscillations corresponding to polarization along the Z axis turn out to be anomalously low.)

It is interesting that the tendency of the metallic phase of hydrogen to form families of structures differing very little in energy pertains not only to the lowest value of the system energy. The next aggregate of close minima, corresponding to tetragonal-symmetry lattices, also turns out to form a family of structures, whose characteristic features is now a fixed quadratic lattice (see Fig. 9b) for the projection of the chains on the basal plane XY. This can easily be verified by analyzing the data pertaining to three tetragonal structures and gathered in Table VII. We again encounter very slight differences in the energy and in the value of Ω_0, and close values of all the elastic moduli. Again the modulus $B_{4'4'}$ turns out to be anomalously low, as is also the square of the optical frequency ω_C^2 with polarization along C for the β-Sn structure. (This lattice is an example of a two-atom lattice belonging to the family.) It is clear that a similar analysis is possible also for this family (compressed lattice, small value of c/a, contribution made by practically only the nearest reciprocal-lattice points in the basal plane, whose positions remain unchanged, etc.), as in the case of the "triangular" family.

Thus, the transition from the optimum modification to a modification that lies higher in energy is actually a transition from a "triangular" to a "quadratic" family of structures.

Attention should be called to the fact that the set of stable or nearly-stable extrema next on the energy scale, which correspond to elongated structures with $c/a > 1$ (see Table I), also has a unique tendency to form a certain unified family. This can be seen best in Table VIII, where all the results are gathered for four entirely different crystal modifications.

Again we have close values of the energies; the distances d_{pl} between the nearest crystal planes along the C axis, as well as the atomic volume Ω_0, are also close in value. It is interesting that in addition to the modulus $B_{4'4'}$, there also appear relatively "soft" moduli B_{66} and B_{33}, corresponding to deformation in the basal plane (with the distance between planes and Ω_0 remaining constant). In comparison with the "triangular" family (see Table VI), these moduli have dropped by at least one order of magnitude. Thus, we are dealing with ease of deformation of the structure in the plane perpendicular to the Z axis. This is why we especially replace $B_{4'4'}$ by the modulus B_{44}, which is defined in terms of the second derivative of the energy with respect to γ_4 (3.5).

It is easy to see that for small deformations $B_{4'4'} = B_{44}$ under the equilibrium condition ($P_2 = 0$), i.e., for the summary value of the modulus. This is not so, however, for the individual contributions to the moduli, since each contribution is realized, as it were, at a corresponding $B_2 \neq 0$. It is all the more interesting to verify that at $c/a > 1$ it is precisely the ionic contribution to B_{44} which becomes small, and furthermore very rapidly with increasing anisotropy (see Fig. 10). Thus, there is a tendency to a relatively weak change of the energy upon deformation of the structure in the plane with the distance between planes maintained constant, and furthermore separately for the ionic and electronic contributions (in the latter case, the greatest role should be played by two fixed close reciprocal-lattice points along the C axis, which dominate by virtue of the elongation of the unit cell). This explains the tendency towards formation of a single family of lattices that differ only in the realignment of the structure

Table VII

Lattice type	Ω_0/a_B^3	c/a	d/a_B	E, Ry/atom	B_{11}	B_{22}	B_{12}	B_{33}	$B_{4'4'}$	B_{66}
PT_1	19.07	0.79	2.289	−1.05866	14.2	20.8	3.7	28.3	−0.2	2.3
FCT_1	18.96	0.40	2.294	−1.05912	14.1	22.0	4.1	27.5	0.8	2.6
β-Sn	19.03	0.39	2.290	−1.05880	13.9	22.1	4.0	27.9	0.2	2.5

Note. $a^2\rho\omega_a^2/16 = 19.4$ and $c^2\rho\omega_c^2/4 \approx -1.0$ for β-Sn.

Table VIII

Lattice type	Ω_0/a_B^3	c/a	d_{pl}/a_B	E, Ry/atom	B_{11}	B_{22}	B_{12}	B_{33}	B_{44}	B_{66}
PH_2	18.48	1.107	2.973	−1.05362	15.6	20.0	−2.5	1.1	0.3	$\equiv B_{33}$
RH	18.41	1.925	2.971	−1.05363	14.7	19.4	−2.9	2.5	0.4	$\equiv B_{33}$
HCP	18.40	2.217	2.966	−1.05346	14.5	19.8	−2.8	2.6	0.5	$\equiv B_{33}$
FCT_2	18.58	1.642	2.931	−1.05230	14.4	21.5	−2.9	−1.1	−0.8	2.7

Note. $a^2\rho\omega_a^2/4 = -1.6$ and $c^2\rho\omega_c^2/4 = 96.1$ for the HCP lattice.

in a plane with a negligible change of dpl and with a low value of the energy barriers between structures (planar family).

It follows from the foregoing analysis that the electron-proton system has in the considered density interval clearly-pronounced tendencies towards formation of strongly anisotropic structures. We note that this result is also obtained when account is taken of the electron-ion interaction only up to terms of second order. But the depth of the minima in this case decreases noticeably. Thus, for the PH lattice the left-side minimum (c/a = 0.69) has a value E = −1.01631, and the right-side minimum (c/a = 1.08) is E = −1.02165. For the HCP lattice, the minimum is located at c/a = 2.12 and equals E = −1.02211. As a result, when the vibrational part of the energy is turned on (see the next section), the cohesion energy (reckoned from the energy of the isolated atoms) becomes positive or close to zero, and this should cause instability of the lattice relative to trivial disintegration into atoms. Thus, inclusion of third-order terms is of fundamental significance here. Physically this is due to the stronger electron-ion interaction at small distances in metallic hydrogen as compared to ordinary metals, which, in turn, is due to the absence of an ionic core. The spatial inhomogeneity of the electron density turns out to be more strongly pronounced than when account is taken of only the second order of perturbation theory, which leads to an increase of the cohesion.

Inclusion of terms of fourth and higher orders will in all probability lead only to a certain further deepening of the minima obtained with allowance for the third order, but the anisotropic picture and the associated tendency to the formation of structure families will be fully retained.

5. PROPERTIES OF GROUND STATE OF METALLIC PHASE OF HYDROGEN. ROLE OF ZERO-POINT OSCILLATIONS

The analysis of the results obtained in the preceding section leads us to the notion of a rather unique structure of the ground state of metallic hydrogen at P = 0. Indeed, if we take the zero-point oscillations into account (or, for example, a temperature of several degrees), then it becomes clear that the individual structures of the obtained family lose their individuality. There should arise, apparently, a single state, which will have the structure of filaments forming a triangular lattice in a plane perpendicular to them, and having no fixed periodicity in space in a direction parallel to the filaments. Thus, we are dealing with a state of matter having only two-dimensional periodicity.

The qualitative picture becomes particularly clear if we consider the role of the long-wave fluctuations in such a system. We introduce the dynamic oscillation matrix $D^{\alpha\beta}(\mathbf{q})$ for a structure corresponding to one of the members of the family, specifically for the primitive hexagonal lattice. If the coordinates of the ions are characterized by two indices m (index of two-dimensional coordinate of the filament) and p (number of the ion along the filament):

$$\mathbf{R}_{mp} = \mathbf{r}_m^0 + \rho_p, \tag{5.1}$$

so that the vector ρ_p is directed along the Z axis, then we have for $D^{\alpha\beta}(\mathbf{q})$

$$D^{\alpha\beta}(\mathbf{q}) = \sum_{m,p} A^{\alpha\beta}_{0m;0p}(e^{-i\mathbf{q}\mathbf{R}_{mp}} - 1). \tag{5.2}$$

Here $A^{\alpha\beta}_{0m,0p}$ is the force matrix, which is determined, as usual, via the second derivatives of the potential energy with respect to the displacements of the corresponding ions.

Let the wave vector of the phonon lie in the basal plane. Then the zz component of the dynamic matrix can be written in the form

$$\begin{aligned} D^{zz}(q_x, q_y, 0) &= \sum_{m,p} A^{zz}_{0m;0p}(e^{-iqr_m} - 1) \\ &= \sum_{m\neq 0}\Big(\sum_{p} A^{zz}_{0m;0p}\Big)(e^{-iqr_m} - 1). \end{aligned} \tag{5.3}$$

This component obviously determines the square of the frequency of the oscillation for the mode with displacement amplitude (polarization) along the Z axis. Recognizing that it is precisely this mode which turns out to be practically equal to zero for an arbitrary value of q in the basal plane, we obtain directly

$$\sum_{p}{}' A^{zz}_{0m;0p} \approx 0 \qquad (m \neq 0). \tag{5.4}$$

Physically, this equality denotes that the shift of the filament as a whole along the Z axis produces no force in this direction for the ions making up the neighboring filaments.

If we now consider the region of arbitrary small wave vectors, i.e., containing already a weak displacement from the basal plane (small q_Z), then we can readily establish, by expanding the dynamic matrix in powers of q_Z, that if (5.4) is strictly equal to zero then the dispersion law of the considered mode with polarization along Z will take the form

$$\omega^2(\mathbf{q}) = \alpha(q_z)^2.$$

From this it follows directly that the mean square of the displacement of an individual ion along the Z axis

$$\langle (u^z)^2 \rangle \sim \sum_{\alpha} \int d^3q \frac{|e_\alpha{}^z|^2}{\omega_\alpha(q)}[2\bar{n}(\mathbf{q},\alpha)+1] \tag{5.5}$$

(e_α is the polarization vector and $\bar{n}(\mathbf{q},\alpha)$ is the Planck distribution for the phonon $\mathbf{q},\alpha$) diverges logarithmically at the lower limit at T = 0 ($\bar{n}$ = 0), and diverges like $1/q_Z$ at T ≠ 0, i.e., exactly as in the purely one-dimensional case.

Let us now find the square of the displacement of the ion in the basal plane. The danger of destroying the two-dimensional structure arises in connection with the vanishing of the modulus B_{44}, or, what is the same, of the velocity of the transverse sound when the phonons propagate along the Z axis. We shall therefore consider specially the phase space near this direction ($\mathbf{n}_Z$ and $\mathbf{n}_\perp$ are unit vectors along Z and in the basal plane):

$$\mathbf{q} = q_z\mathbf{n}_z + \Delta q\mathbf{n}_\perp$$

and analyze the behavior of the dynamic-matrix component

$$D^{xx}(\mathbf{q}) = \sum_{m,p} A^{xx}_{0m;0p}(\exp\{-iq_z\mathbf{n}_z\rho_p - i\Delta q(\mathbf{n}_\perp\mathbf{r}_m)\} - 1). \tag{5.6}$$

At $\Delta q = 0$ this component determines the square of the frequency of the phonon for the mode with polarization along the X axis. The quadratic term of the expansion of the right-hand side of (5.6) in powers of q_Z (at small q_Z) should vanish.

Taking this into account, we can readily conclude from the form of (5.6) that at small q the dispersion law for this mode should be

$$\omega^2(\mathbf{q}) = \alpha_1 q_x^4 + \alpha_2(q_x^2 + q_y^2).$$

If we calculate the mean-squared displacement along the X axis, taking into account the obtained dispersion law, then we verify directly that $\langle (u^X)^2 \rangle$ remains a finite quantity, both for $T = 0$ and $T \neq 0$. Thus, fluctuations do not destroy the regular structure in a plane perpendicular to the filaments.

The results obtained here are in full agreement with the analysis by Landau[24], who was the first to formulate the possibility, in principle, of the existence of bodies whose density function depends on only two coordinates. We note that his analysis implicitly suggested precisely a liquid-like character of motion along Z (and not simply amorphous behavior of the body in this direction, which also leads to $\rho = \rho(x, y)$), which corresponds precisely to the obtained divergence of the squared displacement (5.5).

Thus, the results and qualitative considerations give grounds for assuming that metallic hydrogen in the ground state is a substance made up of proton filaments in an electron fluid, forming a rigid triangular lattice in a perpendicular plane (Fig. 9a) with high frequencies of the transverse oscillations in this plane (Fig. 11), and at the same time with a tendency towards a liquid-like motion in a direction parallel to the filaments.

2. The entire energy analysis above was based on consideration of the static part of the energy. It is clear at the same time that since we are dealing with such a light atom as hydrogen, the vibrational part E_{vib} should also make a noticeable contribution to the total energy. However, as can be easily understood (and as was shown by direct calculations), E_{vib} has practically the same value for all members of one family, and therefore produces no additional energy barriers and consequently does not change the above results. At the same time, the energy gap between the "triangular" and "quadratic" families is increased even more by E_{vib}.

To estimate the zero-point oscillations, we have calculated the phonon frequencies for a number of wave vectors in the first Brillouin zone (at $7 \times 7 \times 7$ points), making it possible to determine with good accuracy the energy of the zero-point oscillations. It was found to be

$$\begin{aligned} E_{vib} &= 0.0168 \text{ for a "triangular" family,} \\ E_{vib} &= 0.0291 \text{ for a "quadratic" family.} \end{aligned} \qquad (5.7)$$

The energy of the zero-point oscillations for structures of a planar family turns out to be even lower than for a triangular family, as a result of the weakening of the shear moduli in the XY plane (see the discussion at the end of the preceding section), but the total energy is as before, higher. (With increasing pressure, the picture may change—details will be reported in the next article.)

It is interesting that, as follows from (5.7), the energy of the zero-point oscillations turns out to be strongly dependent on the structure. It is clear therefore that a certain structureless approximation customarily used for the determination of the E_{vib} (see, for example,[6,7]) is in fact very crude.

In connection with the foregoing results, attention can be called to the following interesting circumstance. The specific character of the potential structure in this system with the simplest interaction leads, in addition to the tendency towards formation of an entire family of crystal structures and by the same token to the appearance of "soft" moduli, also to an overall lowering of the total phonon energy; this lowering is stronger the more sharply pronounced the tendency towards formation of a continuous family. Therefore allowance for E_{vib} only puts the state with the lower energy more definitely into the continuous family of structures.

6. CONCLUDING REMARKS

In the Introduction we have formulated four problems, the solution of which would essentially answer the question of the feasibility and properties of a metastable metallic phase of hydrogen and the fundamental possibility of its production.

The foregoing analysis solves the first two problems. Let us formulate first the results that will remain unchanged when the theory is subsequently quantitatively improved. This pertains primarily to the main result—it should be regarded as established that there exists a metallic phase of hydrogen even at $P = 0$; this phase is locally stable in all the macroscopic parameters and has a large binding energy relative to disintegration into isolated atoms. It was found that in this system with the simplest interparticle interaction, only strongly anisotropic structures are stable. Cubic structures, for example, which are so characteristic of ordinary metals, are absolutely unstable. Anisotropy, in turn, leads to a very interesting fact: there appear families of structures characterized by almost complete absence of energy barriers between structures of one family, and the structures themselves go over into one another by means of a definite type of deformation.

The absolute minimum of the energy turned out to be realizable with the so-called triangular family of structures, which constitutes an aggregate of structures obtained from a primitive hexagonal lattice by shifting the ions parallel to the C axis and conserving the projection in a plane perpendicular to the C axis. There is a tendency here for a unified family to be formed with loss of long-range order along C, but with conservation of a rigid triangular lattice for the projection of the chains in the basal plane. The fact that it is precisely the triangular family that has a minimum with respect to energy can depend, strictly speaking, on the quantitative accuracy of the assumed approximation. It is not very likely, however, that allowance for the next terms of the expansion will change the relative positions of the minima.

The third problem, namely the behavior of the metallic phase under pressure and the question of phase transitions, will be considered in the second part of the paper.

As to the lifetime of the obtained state, which is metastable with respect to a transition to the molecular phase, this question, being purely kinetic and connected with nucleus-formation, remains open. It is interesting that, in principle, owing to quantum effects, this time is finite also at $T = 0$. Unfortunately, one cannot state that the lifetime will be sufficiently large, by virtue of the significant difference between the energies of the metastable phase and of molecular hydrogen at $P = 0$ and the small mass of the hydrogen ions. In this connection, metallic deuterium has undisputed advantages over metallic hydrogen. A factor greatly contributing to the stabilization in the volume is the large difference between the densities of the two phases. (Stability against decay from the surface can be attained by covering the latter with a specially chosen substance.) In this connection, the question of the real dependence of the energy of the molecular phase on the density can become quite critical. It is clear that the lifetime of the metastable state can increase very strongly if we consider in place of $P = 0$ a certain pressure that is finite although much lower than the pressure of the transition from the molecular phase into the metallic one.

We note in conclusion that the results obtained in the present paper should be of considerable interest also for the general theory of metals, since in fact we have considered in detail a certain ideal model of a metal.

[1]E. Wigner and H. B. Huntington, J. Chem. Phys. **3,** 764 (1935).

[2]R. Kronig, J. de Boer, and I. Korringa, Physica (Utrecht) **12,** 245 (1946).

[3]A. A. Abrikosov, Astron. Zh. **31,** 112 (1954).

[4]B. Zh. Davydov, Tr. Geofiz. Inst., Akad. Nauk SSSR **26,** 86 (1955).

[5]V. P. Trubitsyn, Fiz. Tverd. Tela **7,** 3363 (1965) [Sov. Phys. Solid State **7,** 2708 (1966)].

[6]V. P. Trubitsyn, Fiz. Tverd. Tela **8,** 862 (1966) [Sov. Phys. Solid State **8,** 688 (1966)].

[7]T. Schneider, Helv. Phys. Acta **42,** 957 (1969).

[8]A. A. Abrikosov, Zh. Eksp. Teor. Fiz. **39,** 1797 (1960) [Sov. Phys. JETP **12,** 1254 (1961)].

[9]A. A. Abrikosov, Zh. Eksp. Teor. Fiz. **41,** 560 (1961) [Sov. Phys. JETP **14,** 401 (1962)].

[10]A. A. Abrikosov, Zh. Eksp. Teor. Fiz. **45,** 2038 (1963) [Sov. Phys. JETP **18,** 1399 (1964)].

[11]N. W. Ashcroft, Phys. Rev. Lett. **21,** 1748 (1968).

[12]T. Schneider and E. Stoll, Preprint AF-SSR-34, 1969.

[13]E. G. Brovman and Yu. Kagan, Zh. Eksp. Teor. Fiz. **52,** 557 (1967) [Sov. Phys. JETP **25,** 365 (1967)].

[14]Yu. Kagan and E. G. Brovman, Neutron Inelastic Scattering (Proc. Symp. Copenhagen), Vol. 1, Vienna, 1968, p. 3.

[15]E. G. Brovman and Yu. Kagan, Zh. Eksp. Teor. Fiz. **57,** 1329 (1969) [Sov. Phys. JETP **30,** 721 (1970)].

[16]E. G. Brovman, Yu. Kagan, and A. Kholas, Zh. Eksp. Teor. Fiz. 57, 1635 (1969) [Sov. Phys. JETP 30, 883 (1970)].

[17]E. G. Brovman, Yu. Kagan, and A. Kholas, Fiz. Tverd. Tela 12, 1001 (1970) [Sov. Phys. Solid State 12, 786 (1970)].

[18]E. G. Brovman, Yu. Kagan, and A. Kholas, Zh. Eksp. Teor. Fiz. **61,** 737 (1971) [Sov. Phys. JETP **34,** 394 (1972)].

[19]D. Pines and F. Nozieres, Theory of Quantum Liquids, Benjamin, 1966.

[20]W. A. Harrison, Pseudopotentials in the Theory of Metals, Benjamin, 1966.

[21]E. G. Brovman, Yu. Kagan, and A. Kholas, Fiz. Tverd. Tela **13,** ,(1971) [Sov. Phys. Solid State **13,** ,(1972)].

[24]L. D. Landau and E. M. Lifshitz, Statisticheskaya fizika (Statistical Physics), Nauka, 1964, [Addison-Wesley].

Translated by J. G. Adashko
255